ACERP: Vol. 3, No. 2, (Spiring 2017) 45-52

Advanced Ceramics Progress

Research Article

Journal Homepage: www.acerp.ir

Preparation of Cr-doped TiO_2 Thin Film by Sonochemical/CVD Method and its Visible Light Photocatalytic Activity for Degradation of Paraoxon Pesticide

H. Rasoulnezhad[a,b], G. Kavei[a]*, K. Ahmadi[a], M. R. Rahimipour[c]

[a] *Department of Semiconductors, Materials and Energy Research Center (MERC), Karaj, Iran*
[b] *Department of Electrical & Electronics Engineering, Standard Research Institute (SRI), Karaj, Iran*
[c] *Department of Ceramics, Materials and Energy Research Center (MERC), Karaj, Iran*

PAPER INFO

Paper history:
Received 02 August 2017
Accepted in revised form 03 October 2017

Keywords:
Cr-doped
TiO_2
Photocatalyst
chemical vapor deposition
ultrasonic

ABSTRACT

In this work, nanostructured TiO_2 and Cr-doped TiO_2 thin films were deposited on glass substrate through sonochemical-chemical vapor deposition method. The resulting thin films were characterized by X-ray diffraction, Scanning Electron Microscopy (SEM), UV-visible absorption spectroscopy, and photoluminescence spectroscopy techniques. The TiO_2 thin film has nanocubic morphology and the Cr-doped TiO_2 thin film contains nanostructures with irregular shapes in its structures in which these nanostructures themselves are composed of nanorods. Doping the TiO_2 by Cr resulted in a decrease in the band gap energy of TiO_2 and also in the reduction of photogenerated electron-hole recombination rate. The visible light photocatalytic activity of the prepared thin films was also investigated for degradation of paraoxon pesticide. According to the obtained results, the Cr-doped TiO_2 thin film has higher photocatalytic activity than undoped TiO_2 thin film. Moreover, reusability test results revealed that the Cr-doped TiO_2 thin film has higher stability than undoped TiO_2 thin film.

1. INTRODUCTION

Advanced oxidation processes (AOPs) using semiconductor photocatalysts is an effective method for photocatalytic degradation of the organic pollutants because of its potential advantages such as low-cost, sustainable treatment technology, and its environmentally friendly nature [1]. Among the various semiconductors such as ZnO, ZnS, ZnWO4, Fe2O3, Nb2O5, Bi2WO6, WO3, BiTiO3, and SrTiO3, titanium dioxide (TiO_2) is the most important photocatalyst in this field because of its non-toxicity, good photochemical and chemical stability, facile preparations, strong oxidizing power, highest light conversion efficiency, and cheap availability [2-4].

Because of the large band gap energy of TiO_2 (3.2 eV for the anatase phase and 3.0 eV for the rutile phase [5]), its photocatalytic activity is limited to ultraviolet irradiation ($\lambda < 400$ nm), which corresponds to small proportion (3-5%) of solar radiation [6]. For effective solar light utilization in the photocatalytic degradation of organic pollutants on TiO_2, modification of its band-gap energy is necessary for extending the absorption wavelength from the ultraviolet (UV) to the visible light region [7]. Moreover, the separation efficiency of the photoinduced electron-hole on TiO_2 surface must be improved for enhancing its photocatalytic activity [8]. In recent years, different techniques have been developed to decrease the band gap energy of TiO_2, most of which are increasing the porosity of TiO_2 [9], surface modification [10], doping with metal or non-metal ions [11], self-doping [12], co-doping with metal and non-metal ions atoms [13], compositing with carbon nanomaterials such as graphene [14], and sensitizing with narrow band gap semiconductor quantum dots (QDs) or organic dyes [15].

It is well-known that doping the TiO_2 with an appropriate amount of different transition metal ions can create some electron trapping sites in the TiO_2, resulting in a decrease in photogenerated electron-hole recombination rates. Furthermore, presence of metal ions in the structure of TiO_2 decreases the band gap energy of TiO_2. Thus, doping the TiO_2 with metal ions is recognized as an efficient method to improve the visible light-photocatalytic activity of TiO_2 [16]. Among the transition metal ions as dopants, Cr(III) is an interesting one, as it has an ionic radius (0.76 nm) close to that of the Ti(IV) (0.75 nm), so it can easily penetrate into the TiO_2 crystal structure and occupy the position of Ti(IV) in the TiO_2 lattice [17, 18]. Moreover, in by doping TiO_2 with -transition metal ions, a new energy

*Corresponding Author's Email: g-kavei@merc.ac.ir (G. Kavei)

level is formed inside of the band gap energy of TiO_2 resulting in the decrease of its band gap energy and leading to significant enhancement in the visible light photocatalytic activity of TiO_2 [19, 20].

There are many various methods for preparation of Cr-doped TiO_2 thin films like sol-gel [21], arc plasma deposition [22], microwave-assisted sol–gel method [23], RF-sputtering [24], spray pyrolysis [18, 25], molecular beam epitaxy [26], microwave-assisted hydrothermal [27], and microemulsion-mediated solvothermal synthesis [28] methods. However, among these techniques, CVD method has some advantages such as good adhesion of film to substrate, superior surface coverage, high deposition rate, and high uniformity of the prepared thin film [29]. Prasad et al. prepared TiO_2 thin film with nanoparticle morphology by sol-gel method and reported the photocatalytic activity of 0.0069 min−1 for the UV light photocatalytic degradation of paraoxon on it [30]. In sonochemistry, the ultrasound waves were applied directly into the reaction solution for controlling and proceeding of chemical reactions [31]. Furthermore, ultrasound waves could be used as nebulizing agent [32]. Inspired by the above mentioned papers, in this work the TiO_2 and Cr-doped TiO_2 thin films were deposited on glass substrate by a novel combination of sonochemical and chemical vapor deposition (CVD) methods for the first time. In the current sonochemical/CVD method, ultrasound waves are used as nebulizer in order to spray the sonochemically prepared TiO_2 or Cr-doped TiO_2 sol solution as small mist particles in which these particles are thermally decomposed in the subsequent CVD chamber to produce the desired thin films.

2. MATERIALS AND METHOD

2.1. Materials

The following chemicals were used in this work without further purification: titanium (IV) butoxide (purity ≥99.9%, Art. No: 8.21084.0500 from Merck), chromium(III) nitrate nonahydrate $Cr(NO_3)_3.9H_2O$ (purity > 98%, Art. No: 1.02481.0250 from Merck), absolute ethanol (99.5% v/v, Art. No: 1.00986.2500 from Merck), and Hydrochloric acid fuming 37% (Art. No: 1.00317.1000 from Merck).

2.2. Preparation of TiO_2 thin films

In this work for preparation of the TiO_2 thin films, at first TiO_2 colloidal suspension (sol) was prepared by dissolving 5 ml titanium (IV) butoxide in 20 ml absolute ethanol, and then a solution mixture containing 20 ml absolute ethanol, 0.2 ml concentrated hydrochloric acid and 0.5 ml deionized water was added in dropwise manner to the titanium (IV) butoxide solution under vigorous stirring. The pH of the final TiO_2 sol solution was adjusted to about 2.1 by addition of concentrated hydrochloric acid. After 18 hours stirring at this condition, the prepared TiO_2 sol solution was transferred into the flask 1 (Fig. 1), and converted to small mist particles by ultrasound waves (produced by Sonicator 3000; Bandeline, MS 72, Germany) as sonochemical and nebulizing agents. In following, the mist particles were carried by argon gas (with flow rate of 60 ml/min) into the flask 2. Flask 2 acts as a sedimentation flask and the large mist particles are settled down inside it, and only very small mist particles moved to Flask 3. For preparing thin films with high monodispersity, the large and small mist particles must be separated for this reason Flask 2 is designed at this position of the deposition setup. Inside the Flask 3 (as a CVD chamber), the migrated mist particles from the previous flask are thermally decomposed at 320°C and TiO_2 thin film is formed on a glass substrate. The procedure for the preparation of Cr doped TiO_2 thin films is same as for TiO_2 thin films preparation except that 54 mg chromium(III) nitrate nonahydrateas a source of chromium was added into the titanium (IV) butoxide solution and the pH of the final TiO_2 sol solution was adjusted to about 2.1 by addition of concentrated hydrochloric acid. The TiO_2 and Cr doped TiO_2 thin films deposited on glass substrate were labeled as TiO_2-G and Cr-TiO_2-G (Table 1), respectively.

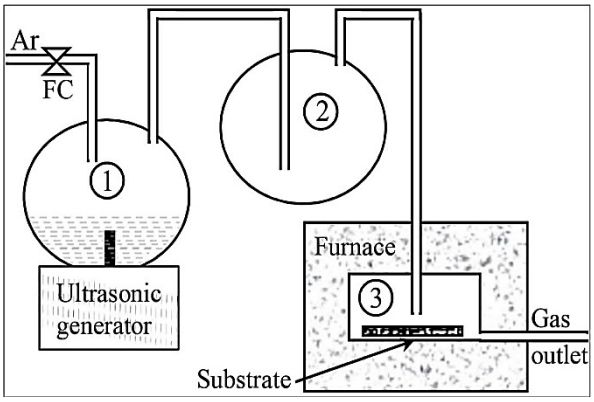

Figure 1. Schematic illustration of the thin film deposition setup.

TABLE 1 Different deposition conditions and sample labels.

Sample label	Cr doping	Deposition temperature	Deposition time	Substrate
TiO_2-G	No	320°C	30 minutes	Glass
Cr-TiO_2-G	Yes	320°C	30 minutes	Glass

2.3. Characterization

X-ray diffraction (XRD) patterns of the prepared thin films were recorded by Philips PW-3710 (Netherlands) X-ray diffractometer with Cu-Kα irradiation (λ=1.54018 Å). Field Emission Scanning Electron Microscopy (FESEM) images and EDS (Energy-dispersive X-ray

spectroscopy) elemental analysis of the prepared samples were acquired by MIRA3 TESCAN field emission scanning electron microscope (Czech Republic). Photoluminescence (PL) emission spectra of the prepared samples were recorded using Cary Eclipse fluorescence spectrophotometer (Varian, Inc., USA) at room temperature, with an excitation wavelength of 320 nm. The UV–visible absorption spectra of the prepared thin films were obtained using Cary 100 Bio spectrophotometer (Varian, Inc., USA).

2.4. Evaluation of the visible light photocatalytic activity of the thin films

To evaluate the visible light photocatalytic activity of the prepared thin film samples in the photocatalytic degradation of paraoxon pesticide, 4 ml of pesticide solution with an initial concentration of 60 mg/L was added to a cuvette containing thin film sample with surface area of 2 cm^2.

Then the cuvette was sealed with glass to prevent the solution evaporation. Before irradiation, the reaction solution was stirred in the dark condition for 24 hours with magnetic stirrer to achieve an adsorption–desorption equilibrium between pesticide and thin film surface. Afterward, a 570 W Xenon lamp (OSRAM Co) as a visible light irradiation source was placed above the reaction solution, and the solution was irradiated at room temperature.

L41 UV cut-off filter (Kenko Co.) with cut-off wavelength of 400 nm was used for elimination of any UV light from the radiation source. To determine the remaining concentration of paraoxon in the solution, the samples were withdrawn from the solution at given time intervals, and the paraoxon concentration was analyzed using a Cary 100 Bio spectrophotometer (Varian).

3. RESULT AND DISCUSSION

3.1. XRD

Fig. 2 shows XRD patterns of the TiO_2-G and Cr-TiO_2-G thin film samples. In XRD pattern of the Cr-TiO_2-G thin film, the diffraction peaks related to the anatase phase of TiO_2 (JCPDS no. 01-083-2243) are appeared at 2θ=25.2, 37.8, 47.9, 54.2, 55.2, 62.7, 68.9, 70.7, and 75.4° corresponding to diffractions from the (101), (004), (200), (105), (211), (204), (116), (220), and (115) planes, respectively. Moreover, there is an extra peak at 2θ=31.7° which can be related to the formation of CrO compound in this sample.

Therefore, the Cr-TiO_2-G sample has anatase crystal structure and CrO compound is formed in its structure. The observed peaks in the XRD pattern of the TiO_2-G thin film are also assigned to the anatase phase of TiO_2, however, because of the amorphous nature of glass substrate some of the peaks related to the TiO_2 are vanished. The sharpness of the diffraction peaks indicates good crystallinity of the thin films.

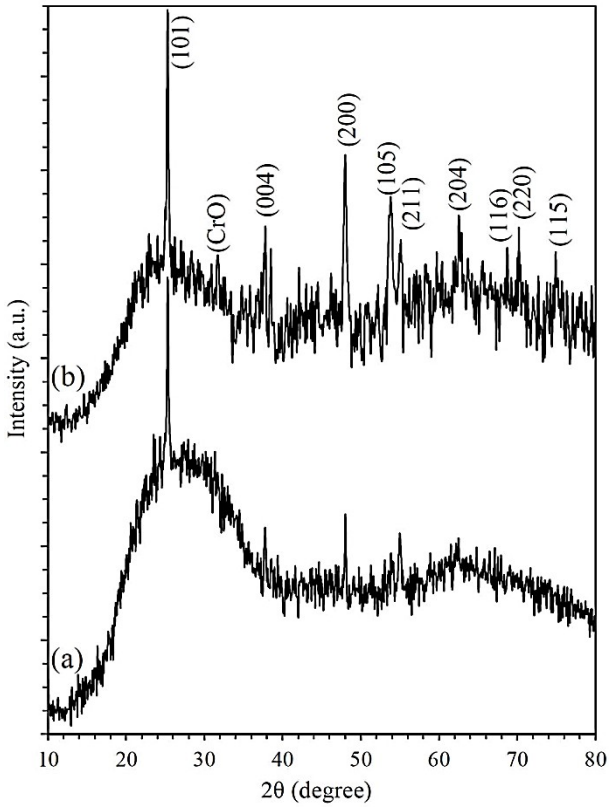

Figure 2. XRD patterns of (a) TiO_2-G and (b) Cr-TiO_2-G thin film samples.

3.2. Surface morphology

Fig. 3 shows the surface morphologies images of the TiO_2-G thin film sample. As this figure reveal, the TiO_2 thin film deposited on glass substrate has nanocubic morphology, and Sizes of these nanoparticles are in the range of 40-80 nm. The high monodispersity of the prepared samples clearly can be seen in Fig. 3(b). As can be seen in Fig. 3(c), the thickness of the TiO_2-G thin film is about 867 nm.

The surface morphologies images of the Cr-TiO_2-G thin film sample are shown in Fig. 4. As can be observed in these images, the Cr doped TiO_2 thin film deposited on glass substrate contains nanostructures with irregular shapes in its structures in which nanostructures with a rod-like structure which has a width of 1–100 nm and an aspect ratio (length/width ratio) between 1 and ~20−25 [33]. As can be seen in Fig. 4(c), the thickness of the Cr-TiO_2-G thin film is about 746 nm.

3.3. EDS

EDS spectra of the TiO_2-G and Cr-TiO_2-G thin films are shown in Fig. 5 (a) and (b), respectively. In the EDS spectrum of the TiO_2-G sample, Ti and O elements, are seen along with the substrate elements. However, in comparison with the EDS spectrum of the TiO_2-G sample, there are additional peaks in the EDS spectrum of the Cr-TiO_2-G sample, which could be related to the Cr element and

indicates successful doping of Cr in the structure of TiO_2. Since soda-lime-silica glass was used as substrate, presence of Ca, Cl, and Na elements in the structure of both samples can be related to the substrate composition.

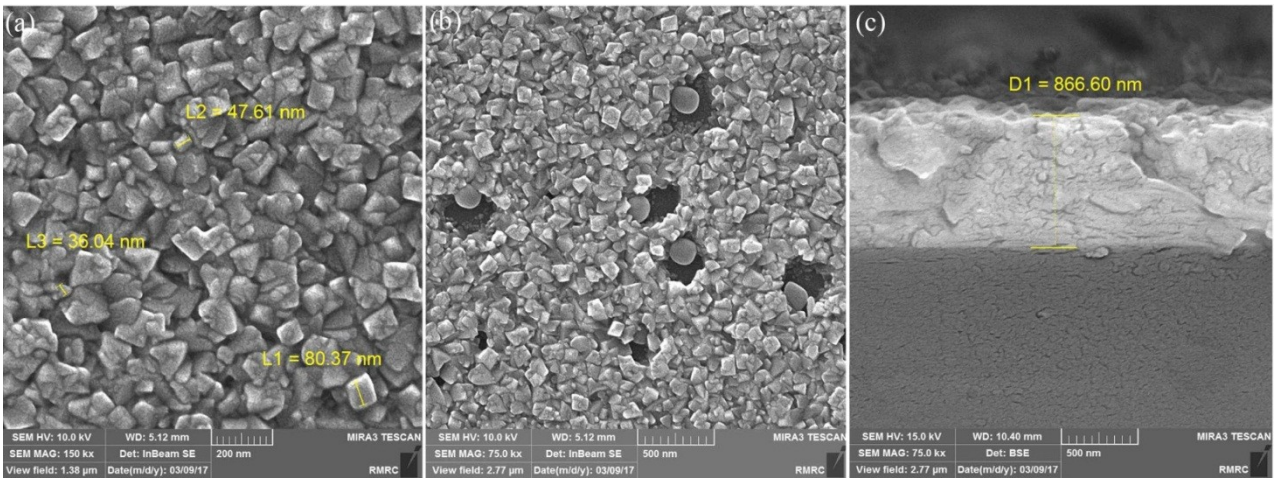

Figure 3. a and b) FE-SEM images of TiO_2-G thin film sample at different magnification of 150kx and 75kx, respectively. c) FE-SEM image from cross-section view of TiO_2-G sample.

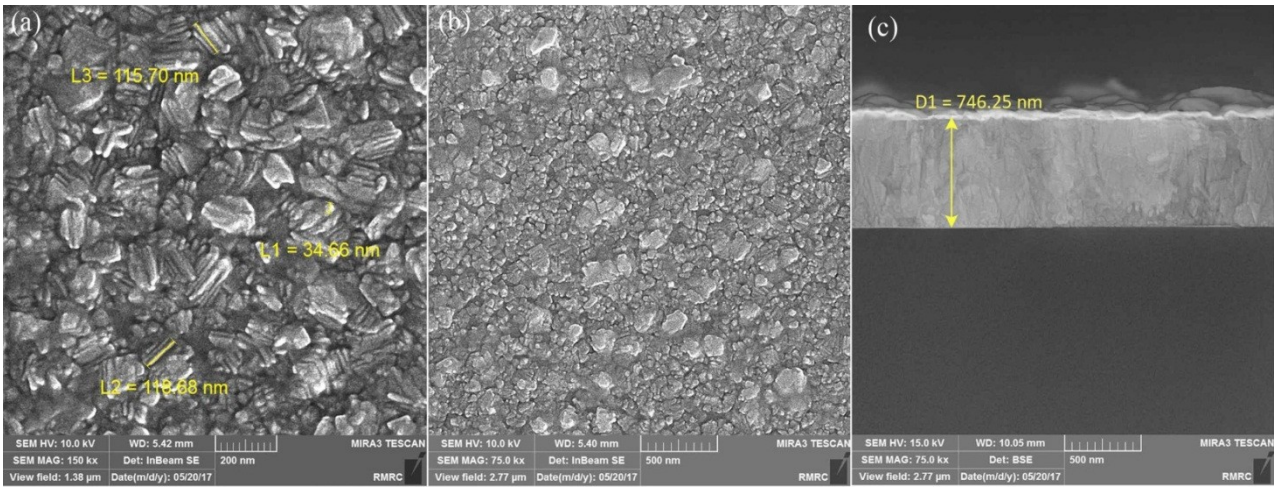

Figure 4. a and b) FE-SEM images of Cr-TiO_2-G thin film sample at different magnification of 150kx and 75kx, respectively. c) FE-SEM image from cross-section view of Cr-TiO_2-G sample.

3.4. Optical Properties

In order to evaluate the effect of the chromium doping on the optical properties of the prepared thin films, UV− visible absorption spectra of these samples were investigated by UV− visible absorption spectroscopy for which the obtained spectra are shown in Fig. 6. As the results of this experiment reveal, the undoped TiO_2 thin film (TiO_2-G sample) has no absorption in visible light region, however, by doping chromium in the structure of TiO_2 (Cr-TiO_2-G sample), a weak absorption in visible region can be observed. Furthermore, in comparison with the absorption spectra of the pure TiO_2 thin film, there is a significant red shift in the absorption edge of Cr-TiO_2-G sample. For TiO_2-based semiconductors, (as an indirect-band-gap semiconductor), the values of the band-gap energy (Eg) of samples can be estimated from the x-intercept of a fitted tangent line to the linear part of the Tauc plots by using Tauc's equation [34, 35]:

$$\alpha h\nu = A(h\nu - E_g)^2 \quad (1)$$

where α, h, ν, A, and E_g refer to the absorption coefficient, Planck's constant, the incident light frequency, constant value, and band-gap energy, respectively. Fig. 6(b) shows the plots of $(\alpha h\nu)^{1/2}$ versus hν (Tauc plots) for the prepared thin films. The band gap energies of the TiO_2-G, and Cr-TiO_2-G thin films were estimated to be 3.22, and 2.92 eV, respectively. Therefore, the presence of chromium in the structure of TiO_2, decreases the band gap energy of TiO_2 for visible

light absorption. The decrease of band gap energy of Cr-doped TiO_2 thin films can be attributed to the formation of a new energy level inside of the band gap energy of TiO_2 [36].

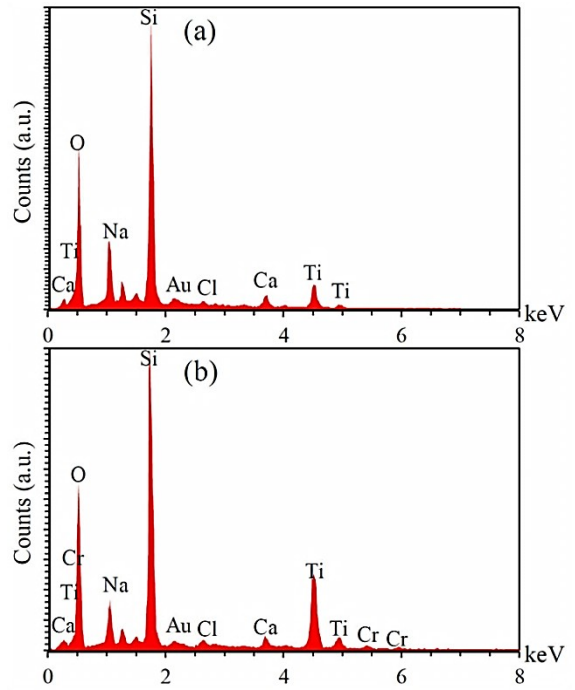

Figure 5. EDS spectra of (a) TiO_2-G and (b) Cr-TiO_2-G thin films.

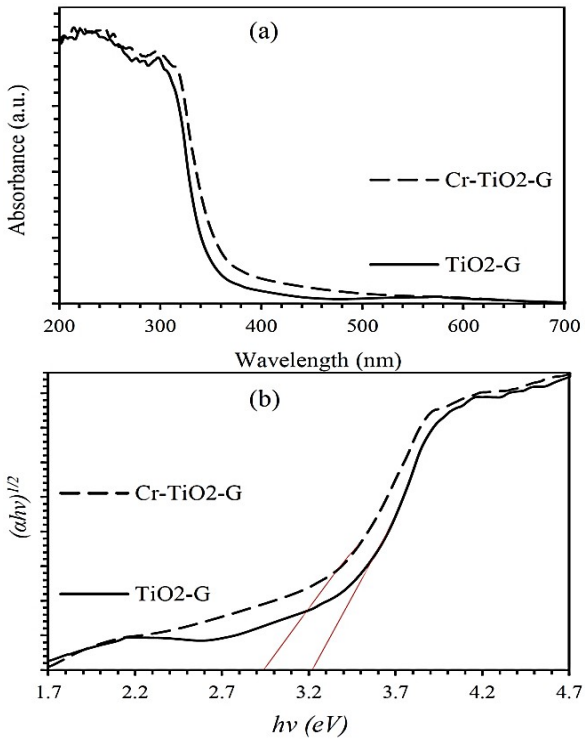

Figure 6. (a) UV-Vis absorption spectra of the prepared thin films samples and (b) band gap energy calculation from Tauc plot.

3.5. Photoluminescence (PL)

Photoluminescence (PL) spectroscopy could be used as an efficient tool in order to get insight into the recombination rate of photo-induced electron-hole pairs [37]. In PL spectroscopy, the PL intensity of a photocatalyst sample is directly proportional to the electron–hole recombination rate on its surface, that is, the higher PL intensity indicates a higher recombination rate, and vice versa [38]. To study the effect of chromium doping on the recombination rate of photo-generated electron-hole pairs, PL spectrum of the Cr-TiO_2-G thin film was compared with that of TiO_2-G sample (Fig. 7). As the results of this experiment in Fig.7, demonstrate, in comparison with TiO_2-G thin film, the Cr-TiO_2-G thin film has lower PL intensity and, consequently, lower electron-hole recombination rate. Therefore, the presence of chromium ions in the structure of TiO_2 decreases electron-hole recombination rate on its surface. Based on the reported works, metal ions in the structure of semiconductor photocatalysts can act as electron trapping centers, and in this way decrease the photogenerated electron-hole recombination rates [16].

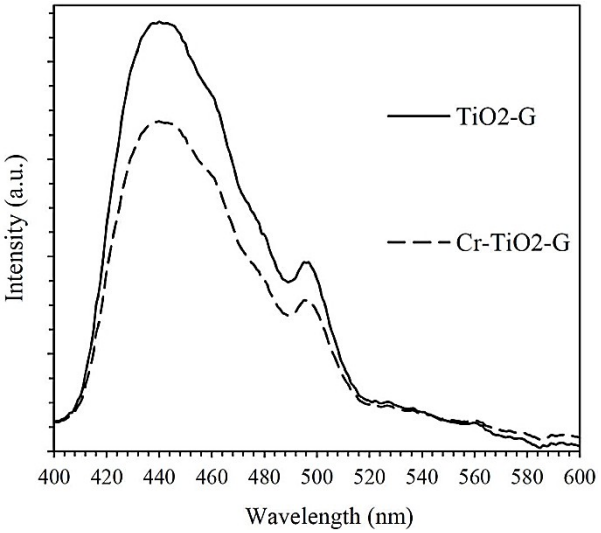

Figure 7. PL spectra of the prepared thin film samples.

3.6. Photocatalytic Activity

The photocatalytic performance of the prepared thin films for visible light photocatalytic degradation of paraoxon can be seen in the C_t/C_0 versus irradiation time plots as shown in Fig. 8 (a), where Ct is the remaining concentration of paraoxon at the irradiation time of t and C0 is its concentration after the adsorption-desorption equilibrium. As this figure indicates, in the absence of any thin film photocatalyst and under visible light irradiation, degradation of paraoxon is negligible, however, when the prepared thin films were added into the paraoxon solution, the photocatalytic degradation of paraoxon was improved significantly.

Due to the low initial concentration of the paraoxon in solution, its photocatalytic degradation kinetic data was well fitted to pseudo-first-order model, and therefore, the reactions rate constants (k) can be calculated using this model. Based on this kinetic model, the reaction rate constants (k) for the photocatalytic degradation of a pollutant were obtained using the following equation:

$$-\ln\left(\frac{C_t}{C_0}\right) = kt \quad (2)$$

The value of the reaction rate constants (k) for visible light photocatalytic degradation of paraoxon over TiO_2-G, and Cr-TiO_2-G thin films can be estimated from the slope of -ln(C_t/C_0) versus irradiation time (t) plots, as shown in Fig. 8 (b). The estimated reaction rate constants for visible light photocatalytic degradation of paraoxon on TiO_2-G, and Cr-TiO_2-G thin films are 0.0052, and 0.0064 min-1, respectively. Based on these results, it can be concluded that between TiO_2-G, and Cr-TiO_2-G thin films, Cr-TiO_2-G thin films have higher photocatalytic activity due to the decrease in their band gap energy and reduced electron-hole recombination rate on their surface.

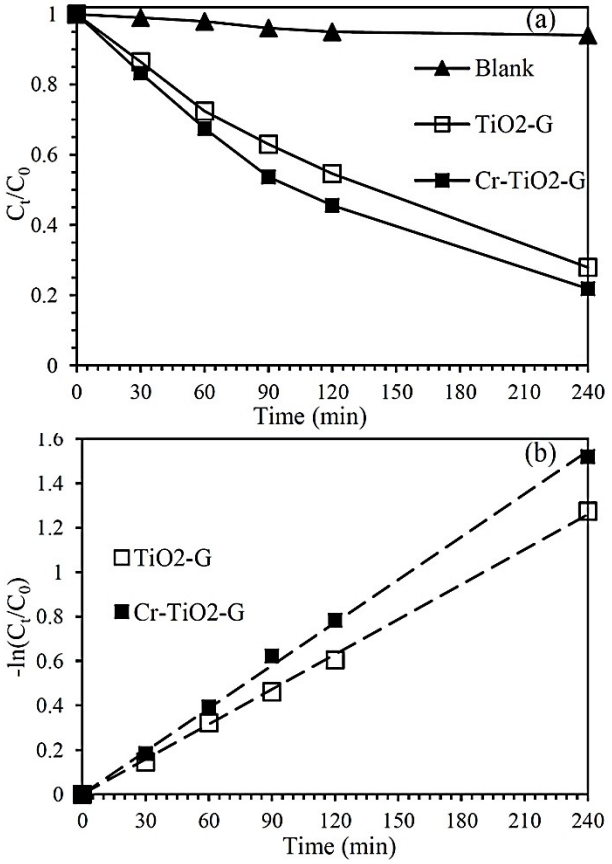

Figure 8. (a) The visible light photocatalytic degradation of paraoxon over the prepared thin films, and (b) calulation of the coresponding reaction rate constants (k) based on the pseudo-first order kinetic model.

One of the important characteristics of photocatalyst systems for practical applications is their stability and reusability under the reaction condition. For this reason, the reusability of TiO_2-G, and Cr-TiO_2-G thin films were examined by a series recycle experiments on the visible light photocatalytic degradation of Paraoxon. After each experiment, the thin films were separated from the reaction solution and washed and dried, and then reused for the next experiment. The results of this experiment are shown in Fig. 9. As this figure demonstrates, the TiO_2-G, thin film maintains 96.4% of its initial activity after three cycles, however, the Cr-TiO_2-G thin film maintains 98.8% of its initial activity after three cycles and there is a slight decrease in its photocatalytic activity. Therefore, incorporating the Cr in the structure of TiO_2 thin film increases its stability, and the Cr-TiO_2-G thin film has higher stability than undoped TiO_2 thin film.

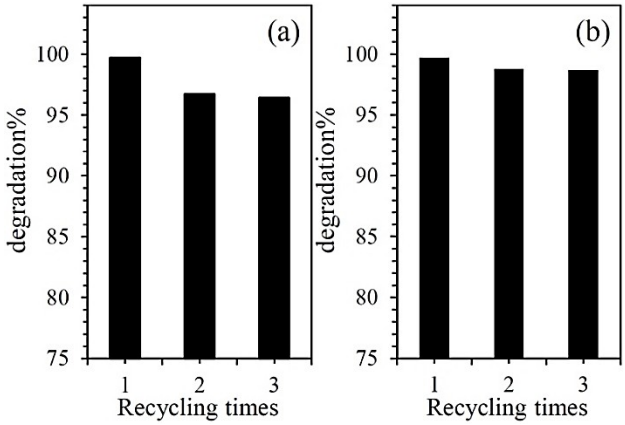

Figure 9. Reusability of (a) TiO_2-G, and (b) Cr-TiO_2-G thin films for visible light degradation of paraoxon.

From the obtained results of this work, it can be concluded that by doping the TiO_2 with Cr, the bond gap energy of TiO_2 and photogenerated electron-hole recombination rate on its surface are decreased. This effect could be related to the formation of a new energy level inside of the band gap energy of TiO_2, resulting in the decrease in its band gap energy and also by trapping of the and photoinduced electron and hole in this energy level, the charge carrier recombination rate is surpassed [19, 20]. For this reason, the Cr doped TiO_2 thin film sample (Cr-TiO_2-G) has higher photocatalytic activity than undoped TiO_2 sample (TiO_2-G). In the case of the photocatalytic degradation of paraoxon pesticide, the photocatalytic activity of Cr-TiO_2-G sample under visible light irradiation (0.0064 min-1) is almost equal with that of TiO_2 thin film under UV light irradiation (0.0069 min-1). Therefore, by doping the TiO_2 with Cr, it is possible to achieve high photocatalytic activity

under visible light irradiation for photocatalytic degradation of organic toxic pollutants.

4. CONCLUSION REMARKS

In summary, in the present work nanostructured TiO_2 and Cr-doped TiO_2 thin films were deposited on glass substrate through sonochemical-chemical vapor deposition (CVD) method and for the first time, were used in the visible light photocatalytic degradation of paraoxon pesticide. The TiO_2 thin film has nanocubic morphology and the Cr-doped TiO_2 thin film contains nanostructures with irregular shapes in its structures in which these nanostructures themselves are composed of nanorods. According to the PL spectroscopy results, between the TiO_2 and Cr-doped TiO_2 thin films, the Cr-doped TiO_2 sample has the lower photoinduced electron-hole recombination rate. In addition, presence of Cr ions in the structure of TiO_2 resulted in a decrease in the band gap energy of TiO_2. According to the obtained results, the visible light photocatalytic activity of TiO_2-G, and Cr-TiO_2-G thin films for degradation of paraoxon are 0.0052, and 0.0064 min-1, respectively, therefore, the Cr-doped TiO_2 thin film has higher photocatalytic activity than undoped TiO_2 thin film. Moreover, in comparison with the undoped TiO_2 thin film, the Cr-doped TiO_2 thin film has higher stability.:

REFERENCES

1. Chong, M.N., Jin, B., Chow, C.W., Saint, C., "Recent developments in photocatalytic water treatment technology: a review", ***Water Research***, Vol. 44, No. 10, (2010), 2997-3027.
2. Chen, X., Mao, S.S., "Titanium dioxide nanomaterials: synthesis, properties, modifications, and applications", ***Chemical Reviews,*** Vol. 107, No. 7, (2007), 2891-2959.
3. Devi, L.G., Kavitha, R., "A review on non metal ion doped titania for the photocatalytic degradation of organic pollutants under UV/solar light: role of photogenerated charge carrier dynamics in enhancing the activity", ***Applied Catalysis B: Environmental***, Vol. 140, No. 1, (2013), 559-587.
4. Esfandiari, S., Honarvar Nazari, H., Nemati, A., Kargar Razi, M., Baghshahi, S., "Characterization of Structural, Optical and Hydrophilicity properties of TiO_2 Nano-Powder Synthesized by Sol-Gel Method", ***Advanced Ceramics Progress***, Vol. 2, No. 2, (2016), 1-6.
5. Landmann, M., Rauls, E., Schmidt, W., "The electronic structure and optical response of rutile, anatase and brookite TiO_2", ***Journal of Physics: Condensed Matter***, Vol. 24, No. 19, (2012), 195503.
6. Bhethanabotla, V.C., Russell, D.R., Kuhn, J.N., "Assessment of mechanisms for enhanced performance of Yb/Er/titania photocatalysts for organic degradation: Role of rare earth elements in the titania phase", ***Applied Catalysis B: Environmental***, Vol. 202, No. 1, (2017), 156-164.
7. Khan, M.M., Ansari, S.A., Pradhan, D., Ansari, M.O., Lee, J., Cho, M.H., "Band gap engineered TiO_2 nanoparticles for visible light induced photoelectrochemical and photocatalytic studies", ***Journal of Materials Chemistry A***, Vol. 2, No. 3, (2014), 637-644.
8. Bian, Z., Tachikawa, T., Zhang, P., Fujitsuka, M., Majima, T., "Au/TiO_2 superstructure-based plasmonic photocatalysts exhibiting efficient charge separation and unprecedented activity", ***Journal of the American Chemical Society,*** Vol. 136, No. 1, (2013), 458-465.
9. Chen, J., Qiu, F., Xu, W., Cao, S., Zhu, H., "Recent progress in enhancing photocatalytic efficiency of TiO_2-based materials", ***Applied Catalysis A: General***, Vol. 495, No. 1, (2015), 131-140.
10. Zuo, F., Bozhilov, K., Dillon, R.J., Wang, L., Smith, P., Zhao, X., Bardeen, C., Feng, P., "Active Facets on Titanium (III)-Doped TiO_2: An Effective Strategy to Improve the Visible-Light Photocatalytic Activity", ***Angewandte Chemie***, Vol. 124, No. 25, (2012), 6327-6330.
11. Roose, B., Pathak, S., Steiner, U., "Doping of TiO_2 for sensitized solar cells", ***Chemical Society Reviews***, Vol. 44, No. 22, (2015), 8326-8349.
12. Zhang, X., Zuo, G., Lu, X., Tang, C., Cao, S., Yu, M., "Anatase TiO_2 sheet-assisted synthesis of Ti^{3+} self-doped mixed phase TiO_2 sheet with superior visible-light photocatalytic performance: roles of anatase TiO_2 sheet", ***Journal of Colloid and Interface Science***, Vol. 490, No. 1, (2017), 774-782.
13. Song, J., Wang, X., Bu, Y., Wang, X., Zhang, J., Huang, J., Ma, R., Zhao, J., "Photocatalytic enhancement of floating photocatalyst: Layer-by-layer hybrid carbonized chitosan and Fe-N-codoped TiO_2 on fly ash cenospheres", ***Applied Surface Science***, Vol. 391, No. 1, (2017), 236-250.
14. Keihan, A.H., Hosseinzadeh, R., Farhadian, M., Kooshki, H., Hosseinzadeh, G., "Solvothermal preparation of Ag nanoparticle and graphene co-loaded TiO_2 for the photocatalytic degradation of paraoxon pesticide under visible light irradiation", ***RSC Advances***, Vol. 6, No. 87, (2016), 83673-83687.
15. Sun, W.-T., Yu, Y., Pan, H.-Y., Gao, X.-F., Chen, Q., Peng, L.-M., "CdS quantum dots sensitized TiO_2 nanotube-array photoelectrodes", ***Journal of the American Chemical Society***, Vol. 130, No. 4, (2008), 1124-1125.
16. Schneider, J., Matsuoka, M., Takeuchi, M., Zhang, J., Horiuchi, Y., Anpo, M., Bahnemann, D.W., "Understanding TiO_2 photocatalysis: mechanisms and materials", ***Chemical Reviews***, Vol. 114, No. 19, (2014), 9919-9986.
17. Peng, Y.-H., Huang, G.-F., Huang, W.-Q., "Visible-light absorption and photocatalytic activity of Cr-doped TiO_2 nanocrystal films", ***Advanced Powder Technology***, Vol. 23, No. 1, (2012), 8-12.
18. Tian, B., Li, C., Zhang, J., "One-step preparation, characterization and visible-light photocatalytic activity of Cr-doped TiO_2 with anatase and rutile bicrystalline phases", ***Chemical Engineering Journal***, Vol. 191, No. 1, (2012), 402-409.
19. Ould-Chikh, S., Proux, O., Afanasiev, P., Khrouz, L., Hedhili, M.N., Anjum, D.H., Harb, M., Geantet, C., Basset, J.M., Puzenat, E., "Photocatalysis with Chromium-Doped TiO_2: Bulk and Surface Doping", ***ChemSusChem***, Vol. 7, No. 5, (2014), 1361-1371.
20. Li, X., Guo, Z., He, T., "The doping mechanism of Cr into TiO_2 and its influence on the photocatalytic performance", ***Physical Chemistry Chemical Physics***, Vol. 15, No. 46, (2013), 20037-20045.
21. Bsiri, N., Zrir, M., Bardaoui, A., Bouaïcha, M., "Morphological, structural and ellipsometric investigations of Cr doped TiO_2 thin films prepared by sol–gel and spin coating", ***Ceramics International***, Vol. 42, No. 9, (2016), 10599-10607.
22. Chan, M.-H., Ho, W.-Y., Wang, D.-Y., Lu, F.-H., "Characterization of Cr-doped TiO_2 thin films prepared by

cathodic arc plasma deposition", ***Surface and Coatings Technology***, Vol. 202, No. 4, (2007), 962-966.

23. Mendiola-Alvarez, S., Guzmán-Mar, J., Turnes-Palomino, G., Maya-Alejandro, F., Hernández-Ramírez, A., Hinojosa-Reyes, L., "UV and visible activation of Cr (III)-doped TiO_2 catalyst prepared by a microwave-assisted sol–gel method during MCPA degradation", ***Environmental Science and Pollution Research***, Vol. 24, No. 14, (2017), 12673-12682.
24. Jun, T.H., Lee, K.S., "Cr-doped TiO_2 thin films deposited by RF-sputtering", ***Materials Letters***, Vol. 64, No. 21, (2010), 2287-2289.
25. Ravidhas, C., Anitha, B., Raj, A.M.E., Ravichandran, K., Girisun, T.S., Mahalakshmi, K., Saravanakumar, K., Sanjeeviraja, C., "Effect of nitrogen doped titanium dioxide (N-TiO_2) thin films by jet nebulizer spray technique suitable for photoconductive study", ***Journal of Materials Science: Materials in Electronics***, Vol. 26, No. 6, (2015), 3573-3582.26.
26. Osterwalder, J., Droubay, T., Kaspar, T., Williams, J., Wang, C.M., Chambers, S.A., "Growth of Cr-doped TiO_2 films in the rutile and anatase structures by oxygen plasma assisted molecular beam epitaxy", ***Thin Solid Films***, Vol. 484, No. 1, (2005), 289-298.
27. Lin, H.-y., Shih, C.-y., "Efficient one-pot microwave-assisted hydrothermal synthesis of M (M= Cr, Ni, Cu, Nb) and nitrogen co- doped TiO_2 for hydrogen production by photocatalytic water splitting", ***Journal of Molecular Catalysis A: Chemical***, Vol. 411, No. 1, (2016), 128-137.
28. Jovani, M., Domingo, M., Machado, T.R., Longo, E., Beltrán-Mir, H., Cordoncillo, E., "Pigments based on Cr and Sb doped TiO_2 prepared by microemulsion-mediated solvothermal synthesis for inkjet printing on ceramics", ***Dyes and Pigments***, Vol. 116, No. 1, (2015), 106-113.
29. Morosanu, C.E., Thin films by chemical vapour deposition, Elsevier, (2013).
30. Prasad, G., Ramacharyulu, P., Kumar, J.P., Srivastava, A., Singh, B., "Photocatalytic degradation of paraoxon-ethyl in aqueous solution using titania nanoparticulate film", ***Thin Solid Films***, Vol. 520, No. 17, (2012), 5597-5601.
31. Mason, T.J., Lorimer, J.P., Applied sonochemistry: the uses of power ultrasound in chemistry and processing, Wiley-VCH Verlag GmbH Weinheim, (2002).
32. Cewers, G., Ultrasonic nebulizer, Google Patents, (2002).
33. Moussawi, R.N., Patra, D., "Synthesis of Au Nanorods through Prereduction with Curcumin: Preferential Enhancement of Au Nanorod Formation Prepared from CTAB-Capped over Citrate-Capped Au Seeds", ***The Journal of Physical Chemistry C***, Vol. 119, No. 33, (2015), 19458-19468.
34. Tauc, J., "Absorption edge and internal electric fields in amorphous semiconductors", ***Materials Research Bulletin***, Vol. 5, No. 8, (1970), 721-729.
35. Wu, G., Nishikawa, T., Ohtani, B., Chen, A., "Synthesis and characterization of carbon-doped TiO_2 nanostructures with enhanced visible light response", ***Chemistry of Materials***, Vol. 19, No. 18, (2007), 4530-4537.
36. Yang, K., Dai, Y., Huang, B., "Density Functional Characterization of the Electronic Structure and Visible-Light Absorption of Cr-Doped Anatase TiO_2", ***ChemPhysChem***, Vol. 10, No. 13, (2009), 2327-2333.
37. Wang, H., Lin, H., Long, Y., Ni, B., He, T., Zhang, S., Zhu, H., Wang, X., "Titanocene dichloride (Cp_2 $TiCl_2$) as a precursor for template-free fabrication of hollow TiO_2 nanostructures with enhanced photocatalytic hydrogen production", ***Nanoscale***, Vol. 9, No. 5, (2017), 2074-2081.
38. Liqiang, J., Yichun, Q., Baiqi, W., Shudan, L., Baojiang, J., Libin, Y., Wei, F., Honggang, F., Jiazhong, S., "Review of photoluminescence performance of nano-sized semiconductor materials and its relationships with photocatalytic activity", ***Solar Energy Materials and Solar Cells***, Vol. 90, No. 12, (2006), 1773-1787.